USCAP

Check for updates

ARTICLE

Th17/IL-17 induces endothelial cell senescence via activation of NF-κB/p53/Rb signaling pathway

Liang Zhang[1,2,7], Manli Liu[1,2,7], Wenhua Liu[3,7], Chaojie Hu[2,7], Hongqi Li[4], Jie Deng[1,2], Qi Cao[5], Yiping Wang[5], Wei Hu[6✉] and Qing Li[1,2✉]

Cellular senescence is a key mechanism of age-related vascular endothelial dysfunction. Interleukin-17A (IL-17A) is an inflammatory cytokine produced by Th17 cells (a subgroup of helper T cells), which is a key factor in the development of atherosclerosis. However, the effect of IL-17A on the senescence of vascular endothelial cells is still unclear. In this study, we aimed to explore the role of IL-17A on endothelial cell senescence and its signaling pathways associated with senescence. The proportion of Th17 cells in the spleen and the expression levels of IL-17A, IL-6, and vascular cell adhesion molecule-1 (VCAM-1) in mice of different ages were increased with aging. In vitro experiments showed that proliferation was inhibited, senescent β-galactosidase and senescence-associated proteins (p16, p19, p21, and p53) of mouse aortic endothelial cells (MAECs) were increased with IL-17A treatment. Blocking the NF-κB pathway with ammonium pyrrolidinedithiocarbamate (PDTC) successfully inhibited IL-17A-induced expression of senescence-associated proteins. In conclusion, our data reveal a previously unsuspected link between IL-17A and endothelial cell senescence, which was mediated by the NF-κB /p53/Rb pathway.

INTRODUCTION

Aging is characterized by gradual deterioration, dysfunction, and structural changes of cells, tissues, and organs in the human body. It closely relates to the development of various age-dependent chronic diseases, such as diabetes, cancer, and neurodegenerative and cardiovascular diseases. Multiple theories on the aging mechanism have been proposed by previous studies, mainly including oxidative free radicals, telomere shortening, epigenetic modification, longevity genes, and inflammation [1–5]. The p53 protein, which is a specific transcription factor, is involved in the molecular mechanisms of the cell cycle and senescence. Another protein that plays an essential role in the regulation of senescence is Rb, a DNA-binding protein found in the nucleus that promotes cell cycle arrest [6, 7]. NF-κB binds specifically to the κB site of the promoter or enhancer regions of various cytokines and adhesion factors, which regulate cell differentiation, growth, senescence, apoptosis, and inflammatory responses [8].

Endothelial cell senescence is one of the leading causes of vascular structural changes and vascular dysfunction, that are considered the pathological basis of atherosclerosis (AS) and acute coronary syndrome [9, 10]. However, it has been rarely examined whether inflammation links to the process of endothelial cell senescence. T helper-17 (Th17) cells mainly secrete interleukin 17 that induces immune responses in various tissues by stimulating the expression of other inflammatory cytokines, such as IL-6 and chemokines, such as MCP-1, which are in turn crucial for the development of inflammatory and autoimmune diseases [11–13]. As a subtype of CD4$^+$ T helper cells, Th17 cells appear to be pathogenic in AS due to their pro-inflammatory effects [14]. However, the mechanism of Th17 in endothelial senescence remains unclear.

In the present study, we explored the role of Th17/IL-17A in the senescence of vascular endothelial cells and the association between Th17/IL-17A and age-related NF-κB and the p53/Rb signaling pathways.

MATERIALS AND METHODS

Animals

Male C57BL/6 mice were purchased from the Institute of Model Animals of Nanjing University (Nanjing, China) and housed in groups under specific pathogen-free (SPF) conditions. The mice were used at the age of 6–8 weeks (young mice), at the age of 11–13 months (middle-aged mice), or at the age of 18–24 months (old mice). Five mice were housed in each cage and maintained at 25 °C in an atmosphere-controlled room with a 12-h light-dark cycle. In this experiment, we collected 200 µl blood from retro-orbital sinus of mouse after anesthesia with 10 mg/ml ketamine and 1 mg/ml xylazine in 0.9% saline. Then mice were sacrificed by cervical dislocation and tissues were collected. The spleen and aorta of mice were dissected in a sterile environment in the hood. Then the spleen and aorta of mice were dissected in a sterile environment. The study protocol was approved by the Biomedical Ethics Committee of Anhui Provincial Hospital (Hefei, Anhui, China). All handling and management procedures were following the guidelines of experimental animal administration.

[1]Department of Clinical Laboratory, Anhui Provincial Hospital, Anhui Medical University, Hefei, Anhui, PR China. [2]Department of Clinical Laboratory, The First Affiliated Hospital of USTC, Division of Life Science and Medicine, University of Science and Technology of China, Hefei, Anhui, PR China. [3]Department of Neurology, Wuhan No.1 Hospital, Tongji Medical College, Huazhong University of Science and Technology, Wuhan, Hubei, PR China. [4]Geriatric Cardiology Department, Anhui Provincial Hospital, Anhui Medical University, Hefei, Anhui, PR China. [5]The Centre for Transplantation and Renal Research, Westmead Institute for Medical Research, University of Sydney, Sydney, NSW, Australia. [6]Department of Neurology, The First Affiliated Hospital of USTC, Division of Life Sciences and Medicine, University of Science and Technology of China, Hefei, Anhui, PR China. [7]These authors contributed equally: Liang Zhang, Manli Liu, Wenhua Liu, Chaojie Hu. ✉email: andinghu@ustc.edu.cn; liqing-2001@163.com

ELISA assay

Nine serum samples were obtained from each age group. After the mice were anesthetized, 200 μl blood was collected from retro-orbital sinus. IL-17A, IL-6, IL-1β, and VCAM-1 were measured in serum samples using a mouse ELISA kit following the manufacturer's recommendations (Lifespan Biosciences Inc, Seattle, WA). IL-17A, IL-6, IL-1β, and VCAM-1 levels in serum were detected and were normalized to the corresponding protein levels.

H&E staining and immunohistochemical analysis

The expression of VCAM-1, IL-17A, and IL-17RA in the arteries of each age group was detected by immunohistochemical staining ($n = 10$). H&E staining was performed by the recommended method of the instruction manual. Paraffin sections were placed in xylene and in a series of ethanol for dewaxing. The slices were washed with tap water, sliced into hematoxylin staining, washed again with tap water and stained with eosin. Subsequently, the slices were washed with tap water and finally dehydrated in absolute ethanol and xylene and sealed. The sections were viewed with a fluorescence microscope (Nikon, Japan) and analyzed using the Image J software.

Immunohistochemical staining was performed using the recommended method of the instructions. Paraffin sections were deparaffinized and incubated in 3% H_2O_2 in the dark. The sections were repaired with citrate buffer microwave antigen and the blocking solution was added. A total of 100 μl diluted anti-mouse IL-17A (1:200, Abcam, ab91649), Il-17RA (1:200, Abcam, ab218249), and VCAM-1 (1:200, Abcam, ab134047) antibody was added dropwise at 4 °C overnight. The slides were washed with PBST three times. Hundred microliter of biotinylated goat anti-rabbit IgG (Abcam, ab6721) was added dropwise and following incubation at room temperature for 1 h, the DAB solution was added, and the samples were counterstained with hematoxylin. The slides were dehydrated in ethanol and the staining results were observed microscopically.

Cell culture

After the five mice in each age group were sacrificed by cervical dislocation, the thoracic aorta and abdominal aorta were collected, and mouse aortic endothelial cells (MAECs) were isolated and cultured in vitro. The specific method was as follows: the residual blood in the blood vessel was washed with PBS buffer, then the blood vessels were digested with 0.5% collagenase and bathed in water at 37 °C for 30 min. The digested cells were seeded in 6-well culture plates pre-coated with 10 μg/ml fibronectin and grown in endothelial cell medium 1640 with 20% FBS in a humidified atmosphere at 37 °C in the presence of 5% CO_2. When the number of MAECs in each well reaches 5×10^5, the cells were passaged. The third generation of MAECs were used for cell experiments in vitro. CD31 and CD105, endothelial cell specific markers, were detected by flow cytometry for cell identification. Anti-mouse PE-conjugated CD31 antibody (0.125 μg/test, eBioscience; Thermo Fisher Scientific, Inc., 130-111-540), and anti-mouse APC-conjugated CD105 antibody (0.2 μg/test, eBioscience; Thermo Fisher Scientific, Inc., 17-1051-80) were used here.

Direct detection of Th17 cells

The percentage of Th17 cells in mice spleen was detected by flow cytometry. There were ten mice in each group. Fresh spleens were removed from mice, dissociated in 1640 (Gibco, USA) with sterile needles and passed through 40 μm strainer steel mesh screens to yield single-cell suspensions. ACK lysis buffer was added to the solution for 1 min to eliminate red blood cells. Splenic lymphocytes were isolated and resuspended in RPMI 1640 (Gibco, USA) and cell viability was detected by tryphan blue staining and estimated to >95%. IL-17 and CD4, Th17 cell specific markers, were detected by flow cytometry: anti-mouse PE-conjugated IL-17 antibody (0.5 μg/test, eBioscience, 25-7177-82), and anti-mouse FITC-conjugated CD4 antibody (0.5 μg/test, eBioscience, 11-0042-82) were used here.

Induction of Th17 cells and estimation of their number in vitro

The percentage of Th17 cells in mice spleen was detected by flow cytometry. There were ten mice in each group. Spleen single-cell suspension was obtained and immature T cells were classified according to the instructions of the magnetic sorting kit (Miltenyi Biotec, USA). Following centrifugation, the cell density was adjusted to 1×10^6 cells/ml in the intact medium containing 10% FBS. Before magnetic bead sorting, the anti-mouse CD3 (10 μg/ml) was wrapped in U-bottom 96-well plates and coated overnight at 4 °C. The naive T cells were inoculated into U-

bottomed 96 wells and the control group contained only complete medium, whereas the induction group contained 8 μg/ml CD28, 5 ng/ml TGF-β, 40 ng/ml IL-6, 30 ng/ml IL-23, 10 μg/ml anti-IFN-γ, and 10 μg/ml anti-IL-4. The medium was changed every other day and the culture supernatant was drawn. A total of 100 μl fresh medium was added and supplemented with cytokines. The cells were cultured for 5 days and transferred to a 24-well plate in the presence of 2 μl/ml cocktail. Following 5 h of stimulation, the percentage of Th17 cells was measure by flow cytometry as described above.

Cell cycle analysis

Cell cycle analysis was performed following treatment of MAECs with different concentrations of IL-17A and staining with Propidium Iodide (PI) (Nanjing, Jiangsu, China). The stained cells were analyzed by monochrome fluorescence in a lymphocyte gate using a FACS Calibur (BD Biosciences, Heidelberg, Germany).

Western blot analysis

Western blot analysis was used to detect pathway proteins, such as p53, p21, p19, p16, Rb, and NF-κB in MAECs. Initially, total protein was extracted from the cells of each group using RIPA lysis buffer (0.1 M PBS, pH 7.4 containing 1% deoxycholic acid sodium, 0.2% SDS, and protease inhibitors) and the BCA method was used for protein quantification. The protein samples were subsequently electrophoresed on 12% SDS-PAGE gels and transferred onto PVDF membranes. The membranes were blocked with 5% w/v skim milk in TBST (TBS, 0.1% Tween-20) at room temperature for 1 h and incubated with the following primary antibodies overnight: anti-β-actin (1:10,000, Protein-Tech Group, Inc., 20536-1-AP), anti-p53 (1:3000, ProteinTech Group, Inc., 21891-1-AP), anti-p21 (1:800, ProteinTech Group, Inc., 27296-1-AP), anti-p19 (1:800, ProteinTech Group, Inc., 10272-2-AP), anti-p16 (1:1000, ProteinTech Group, Inc., 10883-1-AP), anti-Rb (1:500, ProteinTech Group, Inc., 10048-2-Ig), anti-NF-κB p65 (1:1000, ProteinTech Group, Inc., 10745-1-AP), anti-p-NF-κB p65 (1:1000, Cell Signaling Technology, Inc., #3039). Following washing with PBS, the membranes were incubated with 1:8000 anti-rabbit IgG/HRP secondary antibody (from Zhong Shan Gin Bridge Biotechnology) at room temperature for 2 h, washed three times and the resulting signals were imaged using ECL reagents (Beyotime Institute of Biotechnology, China). For quantitative analysis, the bands were detected with scanning densitometry using Image Lab software (Bio-Rad Company, USA). The experiment was repeated three times.

β-galactosidase (β-gal) staining

β-gal staining was performed using the recommended method of the instruction manual. Following transfer of the cells onto slides, the latter were removed and the cells were fixed with the fixing solution in the kit for 15 min. The fixing solution was removed and the slides were washed with distilled water three times. The slides were subsequently dried on water and the prepared staining solution was added (a.930 μl 1× Staining Solution, b. 10 μl 100× Solution A, c. 10 μl 100× Solution B, d. 50 μl 20 mg/ml X-gal stock solution). Finally, the slides were incubated overnight in a carbon dioxide-free incubator. The plate was sealed with 70% glycerol and stored at 4 °C. Senescence-associated (SA)-β-gal-positive cells were observed under microscopy and over 400 cells were counted in three independent fields.

Immunofluorescence microscopy

MAECs were seeded in 6-well plates with a density of 1×10^5, covered with sterile slides and subsequently fixed at room temperature for 10–15 min with 4% paraformaldehyde. The slides were rinsed with PBS for 5 min × 3 times. The fixed cells were permeabilized with PBS containing 0.5% Triton X-100 for 10 min and rinsed with PBS for 5 min × 3 times again. The nuclei were stained with 1 μg/ml DAPI solution for 5 min. Following PBS washing and sealing, senescence-associated heterochromatic foci (SAHF) were detected using a Carl Zeiss Axioplan 2 fluorescence microscope (Carl Zeiss, Jena, Germany). Fluorescence images were analyzed using the ImageJ software.

Statistical analysis

All statistical analyses were performed using the SPSS software, version 24.0. The data are expressed as mean ± standard deviation (SD). Comparisons between groups were performed using one-way ANOVA with Bonferroni correction. Statistical significance was set at $P < 0.05$.

RESULTS

The aging changes the morphology of the artery and upregulates Th17 cell population and IL-17A, IL-6, VCAM-1

H&E staining indicated that the arterial endothelial cells in the young group were continuous and smooth, while the smooth muscle cells in the middle layer were arranged neatly; both the endothelial cells and smooth muscle cells in the old group were disordered and misarranged. However, the endothelial cells and the smooth muscle cells in the middle-aged group were better than those in the old group (Fig. 1A). During the aging process,
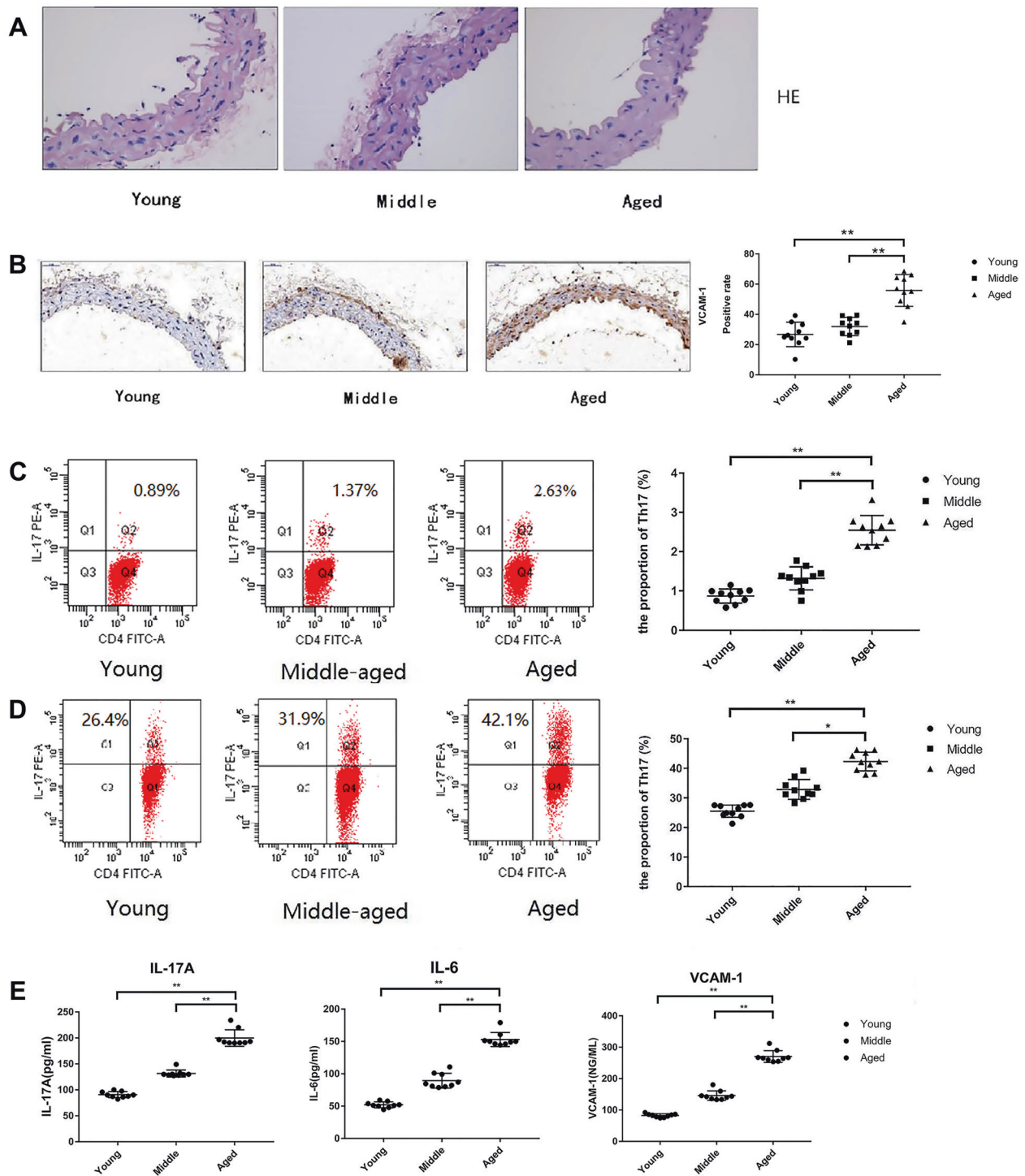

Fig. 1 The morphology of mouse arteries and the expression of Th17 cells and IL-17A, IL-6, VCAM-1 of different age mice. A Hematoxylin-eosin (H&E) staining was performed in order to stain the cytoplasm red and the nucleus blue (Original magnification: ×400). **B** Immunohistochemical staining was used to detect the expression of VCAM-1 in the arteries of young (6–8 weeks), middle-aged (13 months) and old mice (18–24 months) ($n = 10$). The positive areas were stained brown by diaminobenzidine and the negative areas were stained blue by hematoxylin (Original magnification: ×400). **C** The percentage of Th17 cells was detected by flow cytometry in mouse spleen cells following stimulation ($n = 10$). **D** The percentage of the Th17 cells was detected by flow cytometry following induction of spleen cell suspension by Th17 classical induction protocol ($n = 10$). **E** The expression levels of IL-17A, IL-6 and VCAM-1 in the serum were detected by ELISA ($n = 9$). *$P < 0.05$, **$P < 0.01$.

the expression levels of VCAM-1 were significantly higher in the arteries from the old mice than in the arteries in the young and middle-aged mice (Fig. 1B).

The percentage of $CD4^+IL-17^+$ Th17 cells in the spleen cells was directly detected by cocktail stimulation and was estimated to $0.73 \pm 0.18\%$ for young mice, $1.22 \pm 0.15\%$ for middle-aged mice and $2.70 \pm 0.23\%$ for aged mice, respectively. The percentage of Th17 cells was increased with age. The percentage of Th17 cells in aged mice was significantly higher than that in the young and middle-aged groups (Fig. 1C). Subsequently, the spleen cell suspension of each group was induced by the Th17 cell classical induction protocol introduced in methods and materials. The data demonstrated that the change in the percentage of Th17 cells was similar. Following induction, the percentage of Th17 cells in aged mice was $44.01 \pm 7.73\%$, which was significantly higher than that noted in young ($24.02 \pm 4.23\%$) and middle-aged group ($33.86 \pm 6.15\%$) mice (Fig. 1D).

The concentrations of IL-17A, IL-6, and VCAM-1 in the serum of aged mice were increased significantly compared with those noted in the serum of young and middle-aged mice (Fig. 1E). IL-17 is a cytokine secreted by Th17 cells and is an early promoter of T cell-induced inflammatory responses. IL-6 is another aging-related inflammatory factor. In the present study, VCAM-1 was expressed in low levels in the normal state and was mainly localized on the surface of endothelial cells. The three cytokines examined indicated a gradual increase in their levels during aging.

Senescent endothelial cells and senescence-related protein expression in old mice are higher than younger mice

Aortic vessels were removed from young, middle-aged, and old mice for primary endothelial cell culture. The primary endothelial cells of each group were cultured in vitro and were identified by immunocytochemical staining and flow cytometry. The expression levels of von Willebrand Factor (vWF) were detected by immunohistochemistry and the expression of CD31 was measured by flow cytometry. The results indicated that the percentage of endothelial cells in each group was higher than 99% (Fig. 2A).

In addition, the percentage of (SA)-β-gal-positive cells of endothelial cells in old mice was significantly increased than that in young and middle-aged mice according to the results of β-galactosidase staining (Fig. 2B). The SAHF phenomenon of primary endothelial cells in each group was observed, reflecting the degree of endothelial cell senescence. Following DAPI staining, the SAHF phenomenon of primary endothelial cells in old mice was more significant than that noted in young and middle-aged mice as determined by fluorescence microscopy (Fig. 2C).

The primary endothelial cells of each group were collected, and total protein was extracted. The expression levels of aging-related proteins, such as Rb, p16, p19, p21, and p53, were evaluated by western blot analysis. In this experiment, the expression levels of p16, p19, p21, p53, and Rb in aged primary endothelial cells were significantly higher than those in young and middle-aged mice, suggesting that p53/p19/p21 and p16/Rb may be involved in the aging process of endothelial cells (Fig. 2D).

Senescence of MAEC induced by IL-17A in vitro

IL-17A intervention experiments were performed in vitro. We found that when different concentrations of IL-17A were applied to the MAEC line, the percentage of (SA)-β-gal-positive cells, which reflects endothelial cell senescence (Fig. 3A), was significantly increased. Notably, at a concentration of 5 ng/ml, the positive rate of SA-β-GAL was approximately 70%. Subsequently, the total protein of the MAEC treated with different concentrations of IL-17A was extracted, and the expression levels of senescence-associated pathway proteins, such as p53, p19, p21, Rb, and p16 were detected. Following 5 ng/ml of IL-17A intervention, the expression levels of the associated-senescence pathway proteins were significantly increased compared with those in the

non-intervention group (Fig. 3B). Therefore, the concentration of 5 ng/ml was selected for subsequent experiments.

IL-17A intervention on MAEC resulted in a significant increase in IL-17RA expression and in cell cycle arrest

IL-17A exerts an effect by binding to IL-17RA. This binding occurs on the endothelial cell membrane and activates various senescence-related molecular pathways in the cell. The present study demonstrated that the levels of IL-17RA on MAEC were significantly increased following 5 ng/ml IL-17A intervention (Fig. 4A). The expression levels of IL-17A and IL-17RA were significantly higher in the arteries derived from old mouse arteries compared with those of the young and middle-aged mice (Fig. 4B). In addition, the proportion of endothelial cells at the G0/G1 phase was significantly increased following incubation of MAEC with 5 ng/ml IL-17A, which reflected the attenuation of cell proliferation following IL-17A intervention (Fig. 4C).

IL-17A upregulates NF-κB signaling and induces senescence in MAEC in vitro

Subsequently, the expression levels of nuclear factor-κB (nuclear factor-kappaB, NF-κB) were assessed. NF-κB is a cell signaling pathway protein, which acts upstream of p53/Rb. Our results indicated no significant differences in the NF-κB total protein levels in MAEC following the intervention of the cells with 5 ng/ml IL-17A. However, the expression levels of the phosphorylated protein p-NF-κB was significantly elevated compared with those of the control group (Fig. 5A), suggesting that this pathway may be involved in the action of IL-17A.

To explore the role of the NF-κB pathway in the effects of IL-17A on endothelial senescence, we added PDTC (ammonium pyrrolidinedithiocarbamate, an NF-kappa B inhibitor) in the control and IL-17A intervention groups respectively, and observed the changes in the expression levels of each aging pathway protein. The expression levels of p16, p19, and p21 were significantly lower in the IL-17A + PDTC group than those in the IL-17A intervention group (Fig. 5B).

DISCUSSION

Aging results from an accumulation of stress, injury, infection, decline of the immune response and metabolic disorders that lead to a gradual deterioration in cells and tissues. The aging body is generally in a slight state of chronic inflammation and increased serum levels of inflammatory cytokines, such as IL-6, TNF-α, and acute-phase proteins [15, 16]. One of the reasons for chronic inflammation is associated with the aging of our immune system including both the adaptive and the innate types [17]. A low production of naïve T cells that occurs due to thymus involution leads to decreased proliferation of T cells against a stimulus and accumulation of memory T cells by chronic infections [18–20]. In the present study, we explored the association of Th17/IL-17A with vascular endothelial senescence. We provided evidence that the percentages of Th17 cells in the spleen and the concentrations of IL-17A in the serum from aged mice were increased. The expression levels of the senescence-associated proteins and the phosphorylated form of NF-κB were also elevated. The results may suggest that IL-17A induces endothelial cell senescence by NF-κB-related p53/Rb pathway.

Vascular senescence has been the focus of clinical investigations, as it may increase the risk of cardiovascular disease. Previous studies have demonstrated that Th17 and IL-17A play an essential role in infectious and autoimmune diseases [21–23]. Recently, several studies have shown that Th17 and IL-17A are involved in the progression of cardiovascular diseases, such as acute myocardial infarction and cerebral infarction [24–26]. Consistent with the result reported in our previous research, the percentage of Th17 cells and the levels of serum IL-17A in patients with
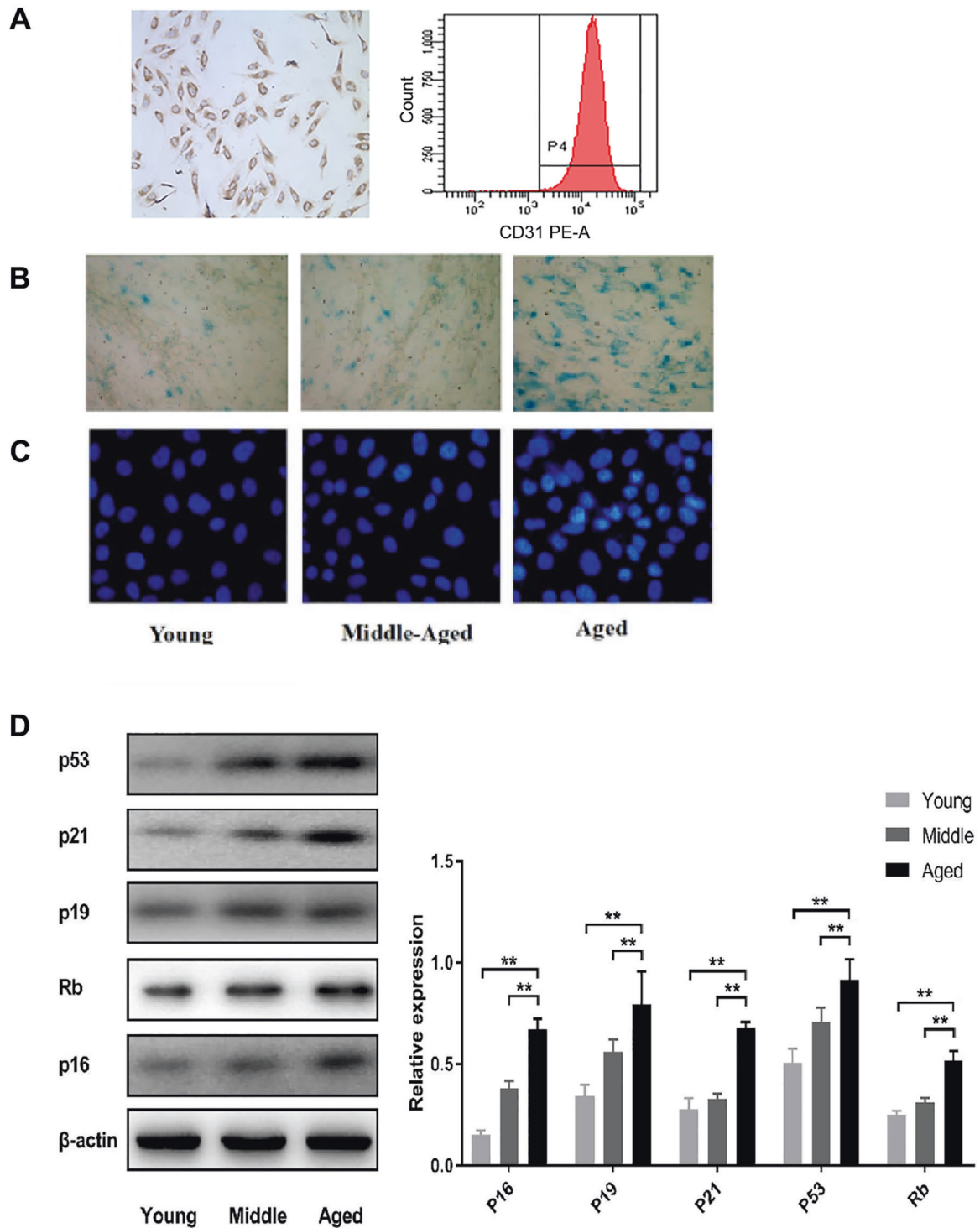
Fig. 2 Immunological identification, senescence staining and SAHF observation of the primary endothelial cells from each group. A The expression levels of vWF and CD31 were detected by immunohistochemistry and flow cytometry. Left: VWF immunocytochemical staining results (Original magnification: ×200); right: flow cytometry analysis. The percentage of endothelial cells in each group was more than 99%. **B** β-galactosidase staining indicated that the percentage of (SA)-β-gal-positive cells in the endothelial cell group of old mice was significantly increased than that in young and middle-aged mice (Original magnification: ×200). **C** DAPI staining and fluorescence microscopy were used to observe the SAHF phenomenon of primary endothelial cells in each group (Original magnification: ×400). **D** The expression levels of senescent proteins were detected by western blot analysis and were significantly increased in arterial endothelial cells of mice of different ages ($n = 3$). **$P < 0.01$.

atherosclerotic cerebral infarction were elevated compared to those of healthy subjects of the same age [27]. The potential mechanism may be attributed to the proinflammatory role of IL-17A in the local inflammation environment on the vessel wall by inducing the production of cytokines and chemokines in endothelial cells or smooth muscle cells, which will in turn recruit neutrophils and monocytes to the inflammatory sites. These factors include IL-6, tumor necrosis factor-α and chemokines, such
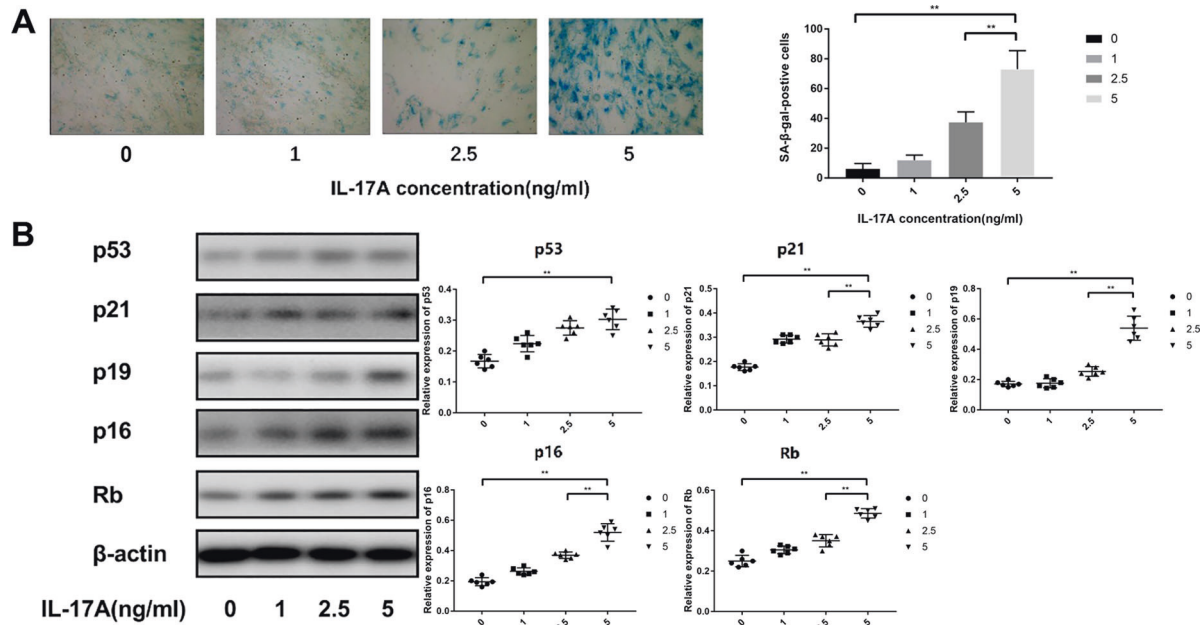
Fig. 3 **Effects of different concentrations of IL-17A on senescence of mouse aortic endothelial cells. A** The senescent cells were stained blue by β-galactosidase staining and the proportion of positive cells in a total number of 400 cells was counted (Original magnification: ×400). **B** Western blot analysis was used to assess the levels of the associated senescence pathway proteins following different concentrations of IL-17A treatment on mouse aortic endothelial cells. ****P < 0.01.**
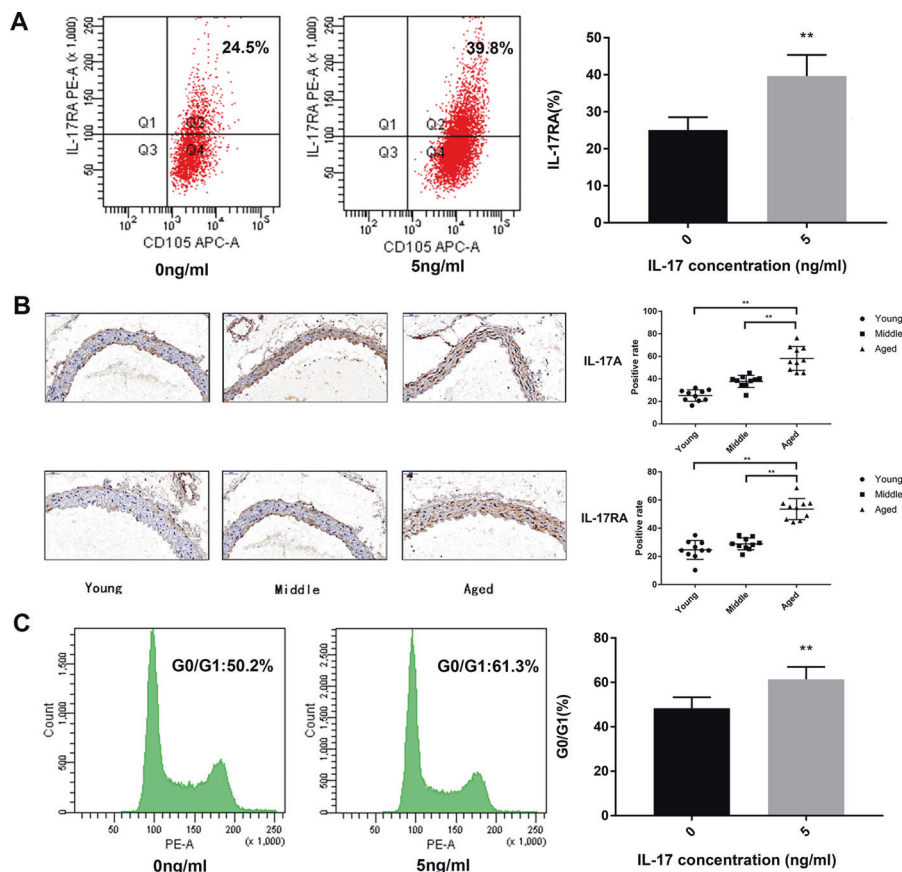

Fig. 4 **Flow cytometry and immunohistochemistry were used to detect the expression levels of the IL-17A/IL-17 receptor A (IL-17RA) and to assess the endothelial cell cycle. A** CD105 was used as an endothelial cell marker molecule. The expression levels of IL-17RA on endothelial cells was detected by flow cytometry. **B** The expression levels of IL-17A/IL-17RA in mice arteries ($n = 10$). The positive areas were stained brown by diaminobenzidine and the negative areas were stained blue by hematoxylin as determined by the results of immunohistochemical staining (Original magnification: ×400). **C** Analysis of the MAEC cell cycle was performed with propidium iodide (PI). The analysis index is the percentage of cells in the G0/G1 phase. ****$P < 0.01$.**
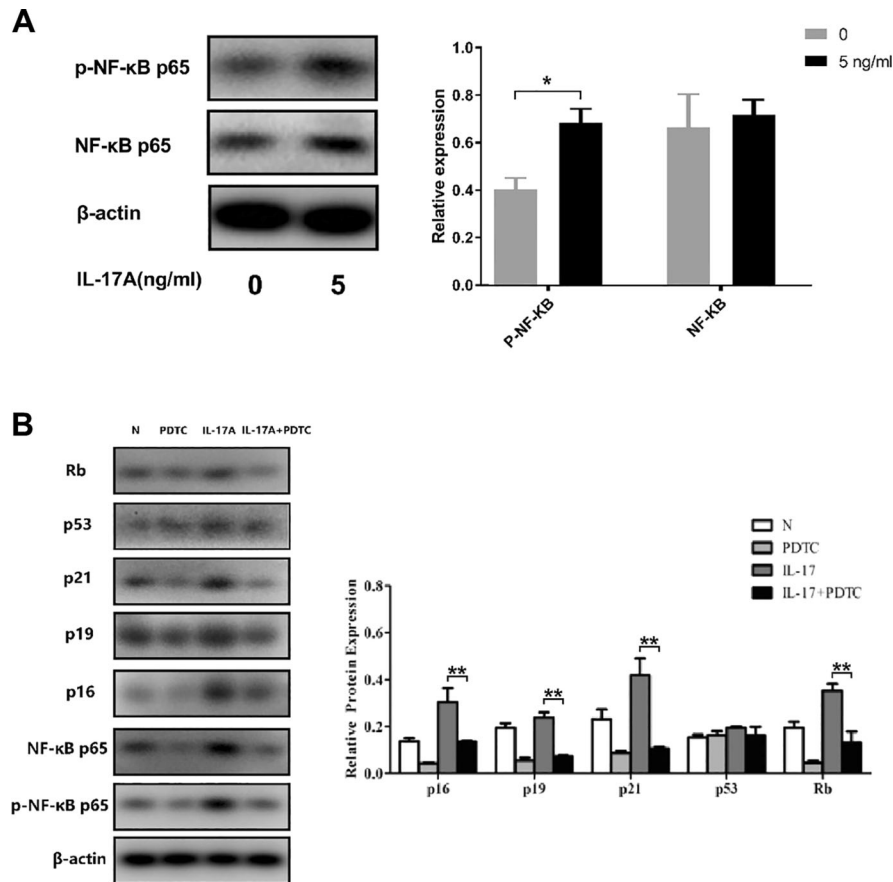
A

B

Fig. 5 **The expression levels of NF-κB, its phosphorylated proteins and those of the p53/Rb senescence pathway proteins were detected by western blot analysis. A** The expression levels of NF-κB and its phosphorylated proteins in MAEC were detected by western blot analysis following incubation with 5 mg/ml IL-17A. **B** The expression levels the senescence proteins in MAEC were detected by western blot analysis following incubation with IL-17A and IL-17A + PDTC, respectively. *$P < 0.05$, **$P < 0.01$.

as CXCL8, CCL2, and CXCL1 [28–30]. In the present study, we found that the expression levels of IL-17A, IL-6, and the vascular cell adhesion molecule VCAM-1 were elevated in peripheral blood samples from healthy aged mice compared to those of young or middle-aged mice. Excessive secretion of IL-6, which is a multi-directional pro-inflammatory cytokine and a key factor in apoptosis, promotes cell cycle arrest and senescence together with p53 and Rb [31, 32]. VCAM-1 is a crucial molecule secreted highly by the endothelium during vascular inflammation. It can participate in the inflammatory response by mediating the adhesion cascade reaction between white blood cells and vascular endothelial cells [33]. The promoter region of the VCAM-1 gene has the binding site of the transcription factor NF-κB that is activated in inflammation [34]. The accumulation of the afore-mentioned inflammatory factors in aged blood vessels is likely to promote age-related functional decline and lead to diseases, such as atherosclerosis.

IL-17RA is widely expressed in epidermal cells, endothelial cells, fibroblasts, macrophages and dendritic cells [35]. It has been reported that IL-17A binds to its receptor and further activates NF-κB through the signal transduction complex IL-17R-Act1-TRAF6 [36]. Our results indicated that the expressions of IL-17RA and phosphorylated NF-κBp65 were elevated in MAEC following IL-17A stimulation, which might suggest that IL-17A binds to IL-17RA on the endothelial cell membrane in order to induce endothelial cell senescence through the NF-κB signaling pathway.

Another prominent feature of senescent cells is the perma-nently arrested state of cell growth. The cell cycle consists of the mitotic phase (M) and the intermitotic phase (G1, S, G2 phase). The

majority of the senescent cells are arrested in the G1 phase of the cell cycle, since a crucial checkpoint determines whether cells can pass from the G1 to the S phase [37]. This checkpoint is mainly executed by the Rb and p53 tumor suppressor pathways. Rb is a nuclear transcription factor that combines the transcription factor E2F before phosphorylation. When Rb is phosphorylated progres-sively by Cdk4/6 complexes it can release E2F, promoting a series of transcription factors necessary for the S phase. p16 is a Cdk4/6 inhibitor, which arrests cells in the G1 phase by indirectly inhibiting Rb phosphorylation [38]. p53 is considered the guardian of the genome, which is activated in response to DNA damage and is responsible for maintaining the genetic integrity in the G1 phase. Once activated, it can trigger the expression of several genes that influence cell cycle arrest and DNA repair. P21, one of the downstream genes of P53, is a cyclin-dependent kinase inhibitor (CDKi), which prevents Rb phosphorylation by inhibiting the activity of cyclin-dependent kinase enzymes. In addition, P19 is also involved in regulating of the cell cycle as an upstream gene of p53. It binds and inhibits mdm2, an ubiquitination ligase that mediates p53 degradation to increase the expression levels of p53 [39]. During the process of senescence, the p19/p53/p21 or the p16/Rb pathways are often activated. In the present study, the expression levels of the key proteins p53, p19, p21, Rb, and p16 in the aged primary endothelial cells were increased significantly compared with those noted in the young mice, indicating that these key proteins did play a role in the aging process. To further explore the mechanism of IL-17A on cell senescence, intervention experiments of IL-17A on MAEC were conducted in vitro. SA-β-GAL activity in MAEC was elevated following the increase in the IL-

17A concentration. The percentage of the G0/G1 phase in endothelial cells was significantly increased following incubation with 5 ng/ml IL-17A. In addition, the expression levels of the proteins p53, p19, p21, Rb, and p16 were also enhanced following an increase in the concentration of IL-17A.

The NF-κB-regulated p53 pathway may contribute to the inflammatory response and cell death [40]. According to our results, the expression levels of p16, p19, p21, and Rb were significantly decreased following induction by PDTC and IL-17A compared with the IL-17A treatment group. The present study demonstrated that NF-κB not only played a role in inflammation but also promoted endothelial cell senescence by regulating the expression of cell cycle-related proteins.

In conclusion, the present study explored the role and mechanism of Th17/IL-17A in endothelial senescence. The percentage of Th17 cells and the expression levels of IL-17A were significantly increased in the aged mice. IL-17A may upregulate the expression levels of IL-17RA on the endothelial cell membrane and further regulate the expression levels of the inflammatory cytokines and cell cycle-related proteins, which are dependent on the NF-κB pathway. This suggested a new IL-17A-dependent pathway that contributes to endothelial senescence via activation of the NF-κB/p53/Rb signaling pathway.

DATA AVAILABILITY
The datasets used during the current study are available from the corresponding author on reasonable request.

REFERENCES

1. Lephart ED. Skin aging and oxidative stress: equol's anti-aging effects via biochemical and molecular mechanisms. Ageing Res Rev. 2016;31:36–54.
2. Everaerts S, Lammertyn EJ, Martens DS, De Sadeleer LJ, Maes K, van Batenburg AA, et al. The aging lung: tissue telomere shortening in health and disease. Respir Res. 2018;19:95.
3. Singh PP, Demmitt BA, Nath RD, Brunet A. The genetics of aging: a vertebrate perspective. Cell. 2019;177:200–20.
4. Chung HY, Lee EK, Choi YJ, Kim JM, Kim DH, Zou Y, et al. Molecular inflammation as an underlying mechanism of the aging process and age-related diseases. J Dent Res. 2011;90:830–40.
5. Huang Y, Hu C, Ye H. Inflamm-aging: a new mechanism affecting premature ovarian insufficiency. J Immunol Res. 2019; 2019:8069898.
6. Rufini A, Tucci P, Celardo I, Melino G. Senescence and aging: the critical roles of p53. Oncogene. 2013;32:5129–43.
7. Singh SK, Banerjee S, Acosta EP, Lillard JW, Singh R. Resveratrol induces cell cycle arrest and apoptosis with docetaxel in prostate cancer cells via a p53/ p21WAF1/ CIP1 and p27KIP1 pathway. Oncotarget. 2017;8:17216–28.
8. Abbas M, Jesel L, Auger C, Amoura L, Messas N, Manin G, et al. Endothelial microparticles from acute coronary syndrome patients induce premature coronary artery endothelial cell aging and thrombogenicity: role of the Ang II/AT1 receptor/NADPH oxidase-mediated activation of MAPKs and PI3-kinase pathways. Circulation. 2017;135:280–96.
9. Sato K, Nuki T, Gomita K, Weyand CM, Hagiwara N. Statins reduce endothelial cell apoptosis via inhibition of TRAIL expression on activated CD4 T cells in acute coronary syndrome. Atherosclerosis. 2010;213:33–39.
10. Sima AV, Stancu CS, Simionescu M. Vascular endothelium in atherosclerosis. Cell Tissue Res. 2009;335:191–203.
11. Giusti D, Bini E, Terryn C, Didier K, Le Jan S, Gatouillat G, et al. NET formation in bullous pemphigoid patients with relapse is modulated by IL-17 and IL-23 interplay. Front Immunol. 2019;10:701.
12. Zhu S, Pan W, Shi P, Gao H, Zhao F, Song X, et al. Modulation of experimental autoimmune encephalomyelitis through TRAF3-mediated suppression of interleukin 17 receptor signaling. J Exp Med. 2010;207:2647–62.
13. Bettelli E, Korn T, Oukka M, Kuchroo VK. Induction and effector functions of T(H)17 cells. Nature. 2008;453:1051–7.
14. Liu Z, Lu F, Pan H, Zhao Y, Wang S, Sun S, et al. Correlation of peripheral Th17 cells and Th17-associated cytokines to the severity of carotid artery plaque and its clinical implication. Atherosclerosis. 2012;221:232–41.
15. Singh T, Newman AB. Inflammatory markers in population studies of aging. Ageing Res Rev. 2011;10:319–29.
16. Weyand CM, Fulbright JW, Goronzy JJ. Immunosenescence, autoimmunity, and rheumatoid arthritis. Exp Gerontol. 2003;38:833–41.
17. Boots AM, Maier AB, Stinissen P, Masson P, Lories RJ, De Keyser F. The influence of ageing on the development and management of rheumatoid arthritis. Nat Rev Rheumatol. 2013;9:604–13.
18. Ginaldi L, De Martinis M, Modesti M, Loreto F, Corsi MP, Quaglino D. Immunophenotypical changes of T lymphocytes in the elderly. Gerontology. 2000;46:242–8.
19. Surh CD, Sprent J. Homeostasis of naive and memory T cells. Immunity. 2008;29:848–62.
20. Nikolich-Zugich J. Ageing and life-long maintenance of T-cell subsets in the face of latent persistent infections. Nat Rev Immunol. 2008;8:512–22.
21. Chang HW, Yan D, Singh R, Liu J, Lu X, Ucmak D, et al. Alteration of the cutaneous microbiome in psoriasis and potential role in Th17 polarization. Microbiome. 2018;6:154.
22. Omenetti S, Bussi C, Metidji A, Iseppon A, Lee S, Tolaini M, et al. The intestine harbors functionally distinct homeostatic tissue-resident and inflammatory Th17 cells. Immunity. 2019;51:77–89.
23. Verstappen GM, Corneth OBJ, Bootsma H, Kroese FGM. Th17 cells in primary Sjogren's syndrome: pathogenicity and plasticity. J Autoimmun. 2018;87:16–25.
24. Zhang L, Wang T, Wang XQ, Du RZ, Zhang KN, Liu XG, et al. Elevated frequencies of circulating Th22 cell in addition to Th17 cell and Th17/Th1 cell in patients with acute coronary syndrome. PLoS ONE. 2013;8:e71466.
25. Ye D, Wang Z, Ye J, Wang M, Liu J, Xu Y et al. Interleukin-5 levels are decreased in the plasma of coronary artery disease patients and inhibit Th1 and Th17 differentiation in vitro. Rev Esp Cardiol. 2019;73:393–402.
26. Luo Y, Zhou Y, Xiao W, Liang Z, Dai J, Weng X, et al. Interleukin-33 ameliorates ischemic brain injury in experimental stroke through promoting Th2 response and suppressing Th17 response. Brain Res. 2015;1597:86–94.
27. Li Q, Ding S, Wang YM, Xu X, Shen Z, Fu R, et al. Age-associated alteration in Th17 cell response is related to endothelial cell senescence and atherosclerotic cerebral infarction. Am J Transl Res. 2017;9:5160–8.
28. Kuwabara T, Ishikawa F, Kondo M, Kakiuchi T. The role of IL-17 and related cytokines in inflammatory autoimmune diseases. Mediat Inflamm. 2017;2017:3908061.
29. Shiotsugu S, Okinaga T, Habu M, Yoshiga D, Yoshioka I, Nishihara T, et al. The biological effects of interleukin-17A on adhesion molecules expression and foam cell formation in atherosclerotic lesions. J Interferon Cytokine Res. 2019;39:694–702.
30. Smith E, Prasad KM, Butcher M, Dobrian A, Kolls JK, Ley K, et al. Blockade of interleukin-17A results in reduced atherosclerosis in apolipoprotein E-deficient mice. Circulation. 2010;121:1746–55.
31. Mosteiro L, Pantoja C, de Martino A, Serrano M. Senescence promotes in vivo reprogramming through p16(INK)(4a) and IL-6. Aging Cell. 2018;17:e12711.
32. Jeon BJ, Yang HM, Lyu YS, Pae HO, Ju SM, Jeon BH. Apigenin inhibits indoxyl sulfate-induced endoplasmic reticulum stress and anti-proliferative pathways, CHOP and IL-6/p21, in human renal proximal tubular cells. Eur Rev Med Pharmacol Sci. 2015;19:2303–10.
33. Kong DH, Kim YK, Kim MR, Jang JH, Lee S. Emerging roles of vascular cell adhesion molecule-1 (VCAM-1) in immunological disorders and cancer. Int J Mol Sci. 2018;19:1057
34. Zhang Q, Lenardo MJ, Baltimore D. 30 Years of NF-kappaB: a blossoming of relevance to human pathobiology. Cell. 2017;168:37–57.
35. Kolls JK, Linden A. Interleukin-17 family members and inflammation. Immunity. 2004;21:467–76.
36. Gaffen SL. Structure and signalling in the IL-17 receptor family. Nat Rev Immunol. 2009;9:556–67.
37. Byun HO, Jung HJ, Seo YH, Lee YK, Hwang SC, Hwang ES, et al. GSK3 inactivation is involved in mitochondrial complex IV defect in transforming growth factor (TGF) beta1-induced senescence. Exp Cell Res. 2012;318:1808–19.
38. Narasimha AM, Kaulich M, Shapiro GS, Choi YJ, Sicinski P, Dowdy SF. Cyclin D activates the Rb tumor suppressor by mono-phosphorylation. Elife. 2014;3:e02872.
39. Kamijo T, Zindy F, Roussel MF, Quelle DE, Downing JR, Ashmun RA, et al. Tumor suppression at the mouse INK4a locus mediated by the alternative reading frame product p19ARF. Cell. 1997;91:649–59.
40. Choi SE, Park YS, Koh HC. NF-kappaB/p53-activated inflammatory response involves in diquat-induced mitochondrial dysfunction and apoptosis. Environ Toxicol. 2018;33:1005–18.

ACKNOWLEDGEMENTS

AUTHOR CONTRIBUTIONS

L.Z., W.H., and Y.P.W. designed and supervised the study; L.Z., M.L.L., C.J.H., and W.H.L. performed animal experiments and in vitro experiments, and analyzed data; Q.L., W.H.L., and H.Q.L. assisted in flow cytometry and provided reagents and expertise; Q.L., Y.P.W., Q.C., J.D., and W.H. participated in discussions, provided intellectual input; L.Z. and M.L.L and wrote the paper. All authors have read and approved the final version of the manuscript.

COMPETING INTERESTS

The authors declare no competing interests.

ADDITIONAL INFORMATION

Correspondence and requests for materials should be addressed to W.H. or Q.L.

Reprints and permission information is available at http://www.nature.com/reprints

Publisher's note Springer Nature remains neutral with regard to jurisdictional claims in published maps and institutional affiliations.